Korean J. Chem. Eng., **26**(2), 587-591 (2009)

Multiple effects of operating variables on the bubble properties in three-phase slurry bubble columns

Ik Sang Shin*, Sung Mo Son*, Uk Yeong Kim*, Yong Kang*,†, Sang Done Kim, and Heon Jung*****

*School of Chemical Engineering, Chungnam National University, Daeduk Science Town, Daejeon 305-764, Korea
**Department of Chemical and Biomolecular Engineering, Korea Advanced Institute of Science Technology, Daejeon 305-701, Korea
***Synfuel Research Group, Korea Institute of Energy Research, Daejeon 305-343, Korea
(*Received 30 July 2008 • accepted 15 October 2008*)

Abstract−Flow properties of gas phase reactants such as size, rising velocity and frequency were investigated in simulated three-phase slurry bubble column reactors. Effects of gas velocity, reactor pressure, liquid viscosity, solid content in the slurry phase and column diameter on the flow properties of a gas reactant were determined. The multiple effects of operating variables on the bubble properties were well visualized by means of contour maps. The effects of operating variables on the flow properties of bubbles changed with changing column diameter of the reactor. The size, rising velocity and frequency of reactant gas bubbles were well correlated in terms of operating variables including column diameter of the reactor.

Key words: Bubble Properties, Slurry Bubble Column Reactor, Pressure, Viscous, Column Diameter

INTRODUCTION

For the production of synthetic liquids such as paraffinic hydrocarbons of variable chain length from syngas or natural gas, various kinds of multiphase reactors have been developed. The three-phase slurry bubble column reactor has been one of the promising schemes for conducting such an energy conversion process, because of its inherent advantages for heterogeneous contacting and reaction. Since the GTL (gas-to-liquid) and CTL (coal-to-liquid) processes and reactors employing slurry bubble columns have been composed of gas-liquid reaction in the presence of catalyst, the effective contacting among three phases has received considerable attention for interfacial mass transfer and the subsequent heterogeneous reaction [1-3].

It has been understood that the chain length distribution of the products could be determined by means of heterogeneous reaction mode and catalyst characteristics. In addition, flow properties of gas phase reactants have been recognized as important factors in determining the reactor performance as well as conversion level in heterogeneous multiphase reactors such as a slurry bubble column reactor for production of liquid fuel from syngas (GTL). Therefore, several investigations have been conducted on the development of slurry bubble column reactors [4-8], however, almost of them were conducted in laboratory scale reactors. For the commercial design or scale-up of the slurry bubble column reactor, an understanding of the flow behavior of bubbles with increasing column diameter is essential, because the similarity of bubble properties should be adjusted with increasing column diameter. It has been generally understood that in dynamic flow systems such as slurry bubble column reactors, the hydrodynamic stability and similarity have to be controlled and adjusted to provide the heterogeneous reactants with plausible conditions for effective contacting and reaction [9-13].

In the present study, thus, effects of column diameter on the flow properties of gas reactants in the slurry bubble column reactor were investigated. In addition, the multiple effects of operating variables on the flow properties of gas bubbles with variation of column diameter were also examined.

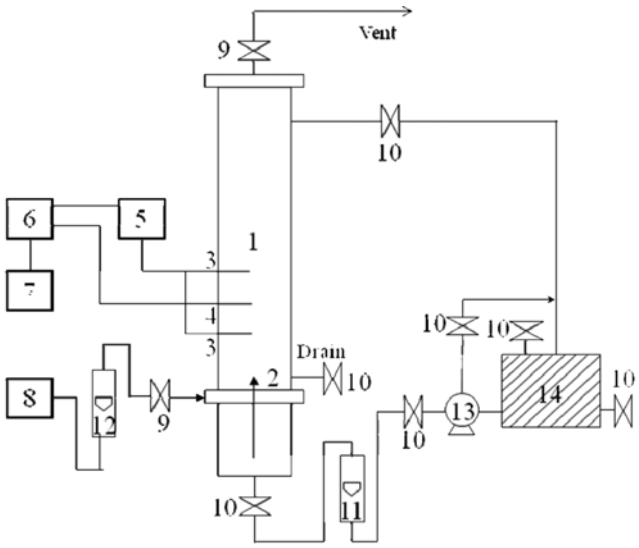

Fig. 1. Schematic diagram of experimental apparatus.

1. Main column	8. Compressor
2. Gas distributor	9. Needle valve
3. Pressure probe	10. Valve
4. Resistivity probe	11. Liquid flowmeter
5. Pressure sensor	12. Gas flowmeter
6. A/D converter	13. Slurry pump
7. Computer	14. Slurry reservoir

†To whom correspondence should be addressed.
E-mail: kangyong@cnu.ac.kr
‡This work was presented at the 7th China-Korea Workshop on Clean Energy Technology held at Taiyuan, Shanxi, China, June 26-28, 2008.

Table 1. Physical and rheological properties of liquid phase

	Dynamic viscosity (mPa·s)	Surface tension (mN/m)	Density (kg/m^3)	K ($Pa \cdot s^n$)	n	Diffusivity (cm^2/s)	Kinematic viscosity (m^2/s)
Water	0.961	72.9	1000	0.001	1	2.22×10^{-5}	9.61×10^{-7}
CMC 0.1 wt%	11	73.2	1001	21.69×10^{-3}	0.882	0.48×10^{-5}	1.10×10^{-5}
CMC 0.2 wt%	24	73.3	1002	43.82×10^{-3}	0.847	0.26×10^{-5}	2.40×10^{-5}
CMC 0.3 wt%	38	73.6	1003	71.69×10^{-3}	0.825	0.19×10^{-5}	3.79×10^{-5}

EXPERIMENTS

Experiments were performed in stainless-steel columns whose inside diameter was either 0.058, 0.076, 0.102 or 0.152 m and 1.5 m in height, as can be seen in Fig. 1. A gas distributor was installed between the main column section and a 0.2 m high stainless-steel distributor box. Oil-free compressed air was fed to the column through a pressure regulator, filter and a calibrated rotameter. It was admitted to the column through 3.0 mm ID perforated pipe drilled horizontally in the grid. The superficial velocity of gas phase ranged from 0.02-0.16 m/s, the pressure ranged from 0.1-1.0 MPa and the viscosity of liquid phase ranged from 1.0-38.0 mPa·s, respectively. The physical properties of the liquid phase are listed in Table 1. Glass bead whose diameter was in the range of 0.4-0.7 μm was used for the slurry phase. The concentration of solid in the slurry phase was in the range of 0-20 wt%.

The bubble size in terms of bubble chord length and frequency was measured by means of a dual electrical resistivity probe system. The probe applied by 1.75 V DC detected the difference in conductivity of gas and liquid. The dual electrical resistivity probe, which was installed at 0.2 m from the distributor, consisted of two 7 mm diameter stainless-steel pipes coated with epoxy resin. The vertical distance between the tips of the two probes was 2 mm. The probe was located at the center between the wall and center of the column. The tips of the probe, which were made of platinum wire, had a diameter of 0.2 mm [14-16].

The analog signals obtained from each probe circuit were processed to produce the digital data. The preselected sampling rate at the personal computer with the DT2805 Lab Card was 500 Hz. The total sampling time was 15 s. The signals were processed off-line. The bubble size (chord length), frequency and holdup were calculated from the relationship between reformed and digitized probe signals and bubble dwell and lag time.

RESULTS AND DISCUSSION

Multiple effects of gas velocity (U_G) and column diameter (D) on the bubble size in three-phase slurry bubble columns can be seen by means of the contour map in Fig. 2. Note in this figure that when the gas velocity was lower than 5 cm/s, the bubble size increased almost linearly with increasing gas velocity and decreased slightly with increasing column diameter. However, when the gas velocity was higher than 6 cm/s, the effects of U_G on the bubble size relatively decreased but the effects of column diameter on the bubble size increased. The influence of column diameter on the bubble size decrease became considerable with increasing gas velocity. This can be due to the fact that the turbulence intensity, owing to the recirculation of continuous liquid slurry medium, would increase with increasing column diameter, which can let bubbles be broken down to smaller bubbles. It has been reported that the recirculation rate of liquid phase in the bubble column increases proportional to the column diameter by $D^{0.3\text{-}0.4}$ [17]. In addition, the turbulent kinematic viscosity in bubble columns has been reported as Eq. (1) [3].

$$\nu_t = 0.036 D^{1.6} U_G^{0.11} \quad (1)$$

The maximum bubble size would exist in the pressurized slurry bubble column reactor without breaking [18,19].

Multiple effects of operating pressure and column diameter on

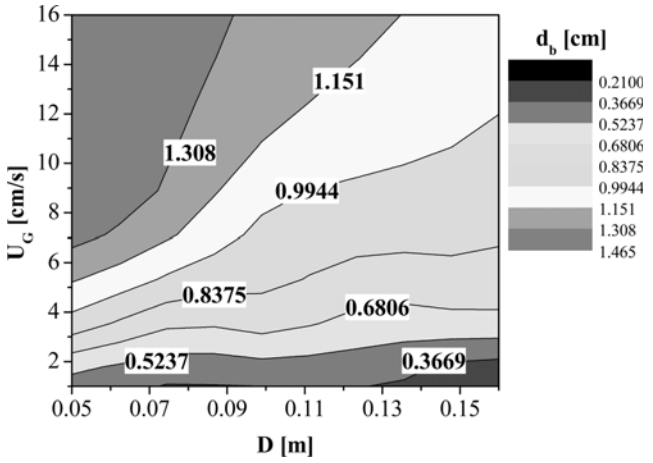

Fig. 2. Contour map of bubble size with variations of U_G & D (S_C= 20 wt%, P=8 kg_f/cm^2, μ_L=24 mPa·s).

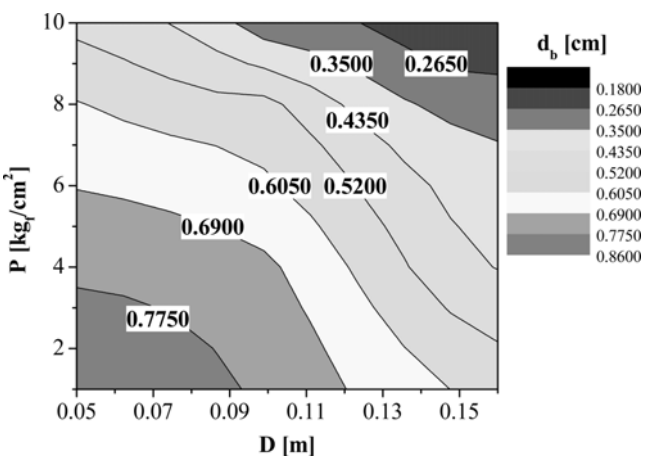

Fig. 3. Contour map of bubble size with variations of P & D (S_C= 20 wt%, U_G=2 cm/s, μ_L=24 mPa·s).

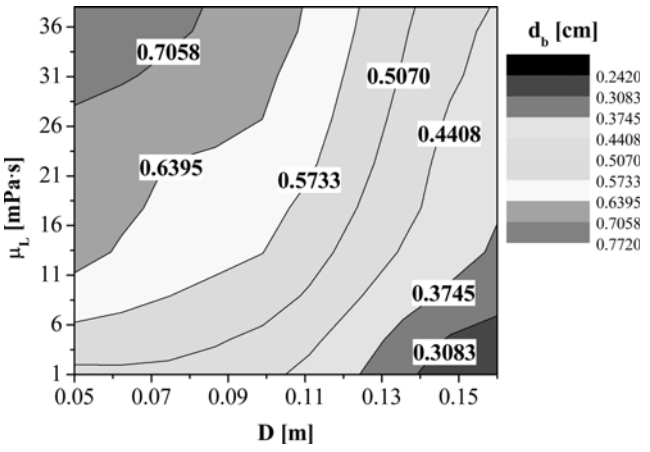

Fig. 4. Contour map of bubble size with variations of μ_L & D (S_C= 10 wt%, U_G=2 cm/s, P=4 kg_f/cm^2).

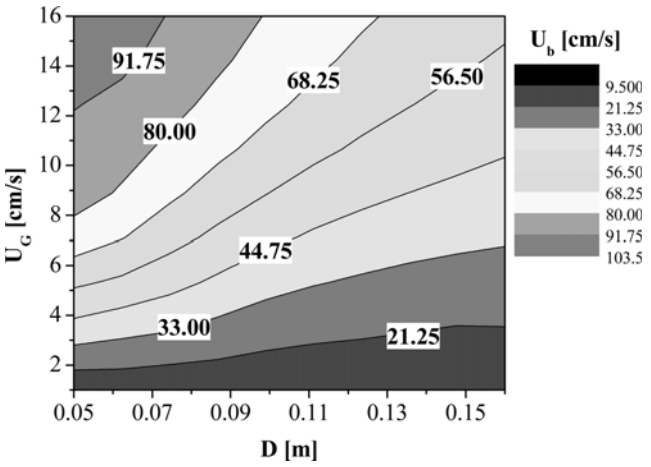

Fig. 6. Contour map of bubble rising velocity with variations of U_G & D (S_C=10 wt%, P=8 kg_f/cm^2, μ_L=24 mPa·s).

the bubble size can be seen in Fig. 3. As expected, the bubble size decreased with increasing operating pressure or column diameter. It can be noted that the decrease trend of bubble size with increasing column diameter is almost linear with the variation of operating pressure. This can be attributed to the fact that the impact force on the gas bubbles in the pressurized slurry bubble column would increase with increasing column diameter, since the pressure is defined by the force per unit area in the column. Multiple effects of liquid viscosity and column diameter on the bubble size can be seen in Fig. 4. In this figure, the bubble size increased with increasing liquid viscosity. The increase ratio of bubble size with liquid viscosity increased with increasing column diameter, although the bubble size in the relatively larger columns was smaller than that in the relatively small columns. This means that the bubble coalescence in the slurry bubble column would increase with increasing column diameter, which can be due to the increase of bubble amount with column diameter in a given superficial gas velocity. Multiple effects of solid concentration and column diameter on the bubble size can be seen in Fig. 5. The bubble size also increased with increasing solid content in the slurry phase. The increase ratio of bubble size with increasing S_C tended to decrease with increasing column diameter.

Multiple effects of gas velocity and column diameter on the bubble rising velocity (U_b) can be seen in Fig. 6. The value of U_b increased with increasing U_G, but decreased with increasing D. Note that the increase ratio of U_b with U_G decreased with increasing column diameter. This implies that the residence time of bubbles in a given superficial gas velocity could increase with increasing column diameter. Especially in the column with relatively large diameter (D≥0.102 m), the increase ratio of U_b with U_G was somewhat decreased with increasing column diameter. Multiple effects of pressure and column diameter on the bubble rising velocity can be seen in Fig. 7, where the value of U_b decreased almost linearly with increasing operating pressure, with variation of column diameter. Multiple effects of liquid viscosity and column diameter on the bubble rising velocity can be seen in Fig. 8. In this figure, the value of U_b increased with increasing liquid viscosity, and the increase ratio was almost linear with variation of column diameter. Multiple effects of S_C and D on the bubble rising velocity can be seen in Fig. 9, where

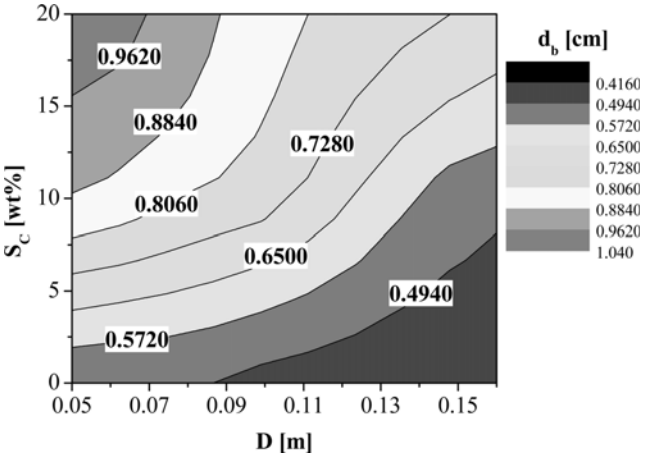

Fig. 5. Contour map of bubble size with variations of S_C & D (μ_L= 24 mPa·s, U_G=4 cm/s, P=8 kg_f/cm^2).

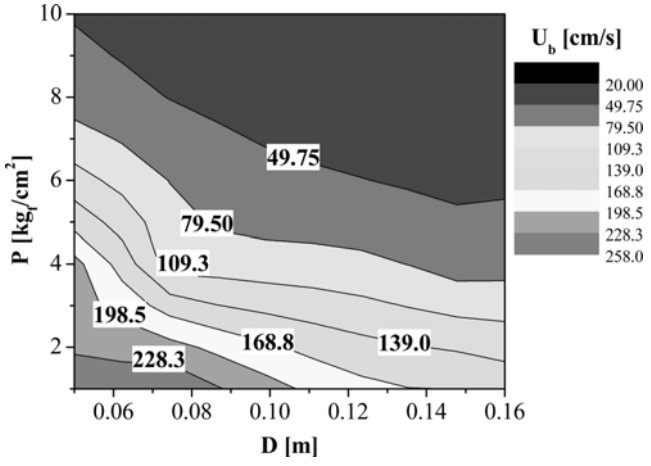

Fig. 7. Contour map of bubble rising velocity with variations of P & D (S_C=20 wt%, U_G=4 cm/s, μ_L=24 mPa·s).

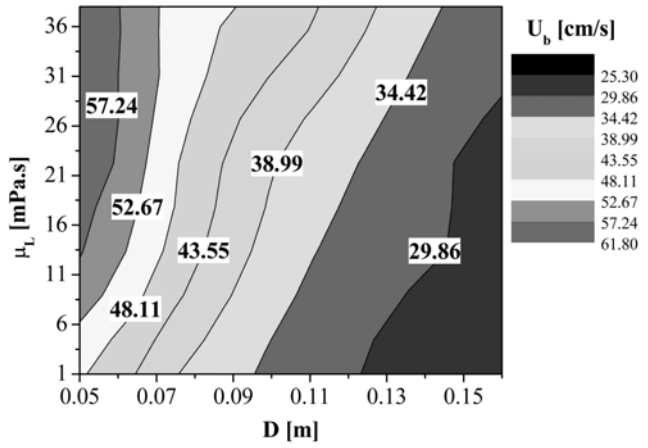

Fig. 8. Contour map of bubble rising velocity with variations of μ_L & D (S_C=20 wt%, U_G=4 cm/s, P=8 kg_f/cm^2).

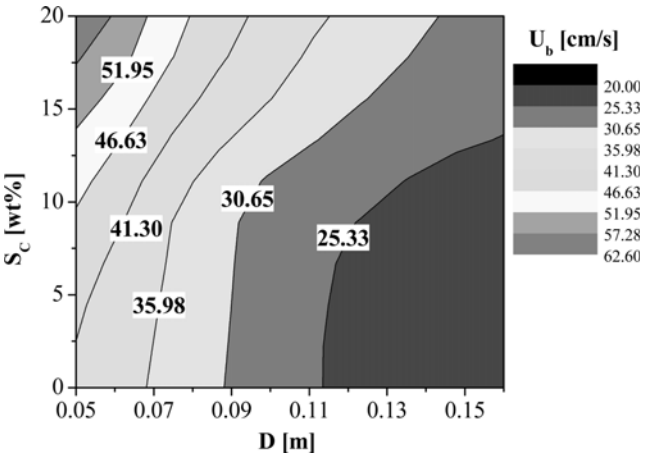

Fig. 9. Contour map of bubble rising velocity with variations of S_C & D (μ_L=24 mPa·s, U_G=4 cm/s, P=8 kg_f/cm^2).

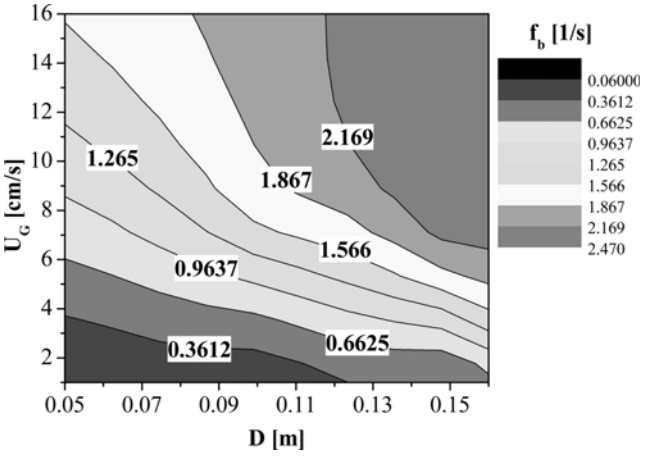

Fig. 10. Contour map of bubble frequency with variations of U_G & D (S_C=20 wt%, P=8 kg_f/cm^2, μ_L=24 mPa·s).

the value of U_b increased with increasing S_C. In this figure, the value of U_b decreased almost linearly with increasing column diameter.

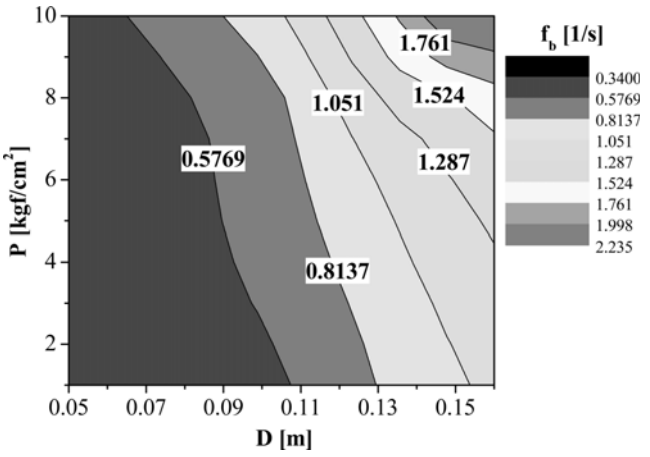

Fig. 11. Contour map of bubble frequency with variations of P & D (S_C=20 wt%, U_G=4 cm/s, μ_L=24 mPa·s).

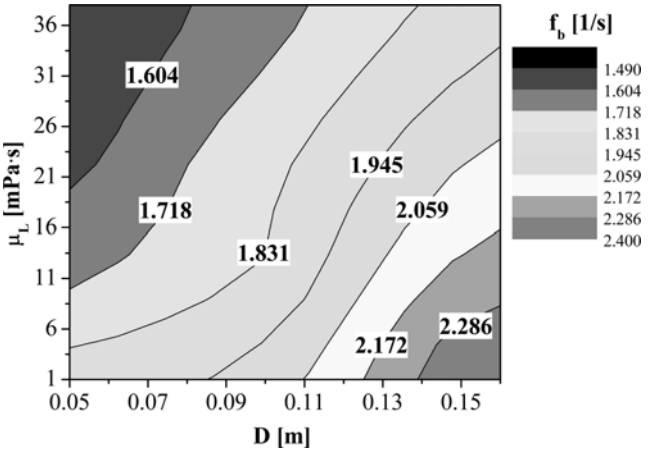

Fig. 12. Contour map of bubble frequency with variations of μ_L & D (S_C=10 wt%, U_G=4 cm/s, P=4 kg_f/cm^2).

Multiple effects of gas velocity and column diameter on the frequency of bubbles (f_b) in slurry bubble column reactors can be seen in Fig. 10. In this figure, the frequency of bubbles increased with increasing gas velocity or column diameter. Note in this figure that the increase ratio of f_b with increasing U_G tended to increase or was sensitive to increasing column diameter. This can be because the amounts of bubbles introduced into the column increase with increasing column diameter at a given superficial gas velocity. Multiple effects of operating pressure and column diameter on the value of f_b can be seen in Fig. 11. In this figure, the value of f_b increased with increasing operating pressure, and the ratio of f_b increased with increasing P became sensitive to increasing D. The value of f_b increased gradually with increasing column diameter. Since the bubble size decreased with increasing P or D in slurry bubble column reactors, as mentioned earlier, the f_b value could increase with increasing P or D in a given gas velocity. Multiple effects of liquid viscosity and column diameter on the bubble frequency can be seen in Fig. 12. In this figure, the value of f_b decreased with increasing liquid viscosity and the decrease ratio of f_b with increasing μ_L tended to increase with increasing column diameter. Multiple effects of solid

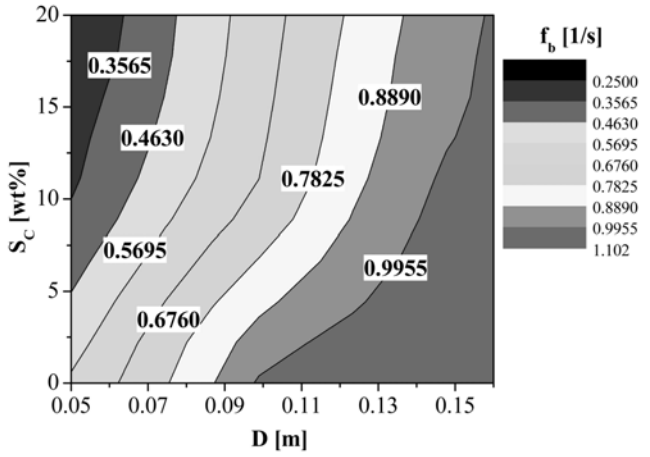

Fig. 13. Contour map of bubble frequency with variations of S_C & D (μ_L=24 mPa·s, U_G=2 cm/s, P=4 kg_f/cm^2).

content in the slurry phase and column diameter on the bubble frequency can be seen in Fig. 13. In this figure, the value of f_b decreased with increasing solid content. This can occur because the bubble size increased with increasing S_C. Note in this figure that the value of f_b increased almost linearly with increasing column diameter.

The bubble size, rising velocity and frequency were well correlated in terms of operating variables as Eqs. (2)-(4), with correlation coefficient of 0.91, 0.98 and 0.94, respectively.

$$d_b=0.11D^{-0.44}U_G^{0.67}P^{-0.31}\mu_L^{0.12}S_C^{0.04} \quad (2)$$

$$U_b=4.47D^{-0.61}U_G^{0.73}P^{-0.82}\mu_L^{0.07}S_C^{0.42} \quad (3)$$

$$f_b=54.36D^{0.89}U_G^{1.14}P^{0.09}\mu_L^{-0.07}S_C^{-1.23} \quad (4)$$

CONCLUSION

The multiple effects of operating variables on the bubble properties such as size, rising velocity and frequency of bubbles were successfully analyzed by means of contour map plotting. The effects of operating variables on the bubble properties were changed with variation of column diameter. The effects of gas velocity on the bubble size decreased, but the effects of column diameter on the bubble size increased, when the gas velocity was higher than 6 cm/s. The decrease trend of bubble size with increasing operating pressure was almost linear with variation of column diameter. The increase ratio of bubble size with increasing μ_L increased with increasing D. The increase ratio of bubble size with increasing S_C tended to decrease with increasing D. The increase ratio of bubble rising velocity with U_G decreased with increasing D. The value of U_b decreased with P, but increased with increasing μ_L almost linearly, with variation of column diameter. The increase ratio of bubble frequency with increasing U_G operating pressure or μ_L became increased with increasing column diameter. The value of bubble frequency increased with increasing column diameter. The bubble properties were well correlated in terms of operating variables.

ACKNOWLEDGMENT

Financial support from Korea Institute of Energy Research (A7-2802) is greatly appreciated.

NOMENCLATURE

D : column diameter [m]
d_b : bubble size [cm]
f_b : frequency of bubbles [1/s]
P : pressure [kg_f/cm^2]
S_C : solid contents [wt%]
U_b : rising velocity of bubbles [cm/s]
U_G : superficial gas velocity [cm/s]

Greek Letters

μ_L : liquid viscosity [mPa·s]
ν_t : turbulent kinematic viscosity [m^2/s]

REFERENCES

1. L.-S. Fan, *Gas-liquid-solid fluidization engineering*, Butterworth Publishers, Stoneham, MA, USA (1989).
2. W.-D. Deckwer, *Bubble column reactors*, John Wiley and Sons, New York (1992).
3. R. Krishna and S. T. Sie, *Fuel Processing Technol.*, **64**, 73 (2000).
4. C. Maretto and R. Krishna, *Catalysis Today*, **52**, 279 (1999).
5. R. Krishna, J. M. van Baten, M. I. Urseanu and J. Ellenberger, *Chem. Eng. Sci.*, **56**, 537 (2001).
6. R. Krishna, J. M. van Baten, M. I. Urseanu and J. Ellenberger, *Chem. Eng. Sci.*, **66**, 199 (2001).
7. J. M. van Baten, J. Ellenberger and R. Krishna, *Catalysis Today*, **79-80**, 259 (2003).
8. A. Forret, J.-M. Schweitzer, T. Gauthier, R. Krishna and D. Schweich, *Chem. Eng. Sci.*, **58**, 719 (2003).
9. K. Zhang and Y. Zhao, *Chem. Eng. Sci.*, **61**, 1459 (2006).
10. A. Behkish, R. Lemoine, L. Sehabiague, R. Oukaci and B. I. Morsi, *Chem. Eng. J.*, **128**, 69 (2007).
11. B. Gandhi, A. Prakash and M. A. Bergougnou, *Powder Technol.*, **103**, 80 (1999).
12. A. A. Mirzaei, M. Faizi and R. Habibpour, *Applied Catalysis*, **306**, 98 (2006).
13. D. J. Duvenhage and T. Shingles, *Catalysis Today*, **71**, 301 (2002).
14. Y. Kang, Y. J. Cho, K. J. Woo and S. D. Kim, *Chem. Eng. Sci.*, **54**, 4887 (1999).
15. Y. Kang, Y. J. Cho, K. J. Woo, K. I. Kim and S. D. Kim, *Chem. Eng. Sci.*, **55**, 411 (2000).
16. S. D. Kim and Y. Kang, *Chem. Eng. Sci.*, **52**, 3639 (1997).
17. J. B. Joshi, U. P. Veera, C. V. Parasad and B. N. Thorat, *PINSA*, **64**, 441 (1998).
18. Y. Wu, B. C. Ong and M. H. Al-Dahhan, *Chem. Eng. Sci.*, **56**, 1207 (2001).
19. X. Luo, D. J. Lee, R. Lau, G. Yang and L. S. Fan, *AIChE J.*, **42**, 665 (1999).